Reactor Physics Calculations for Conversion of McMaster Nuclear Reactor from Use of HEU to LEU fuel

By

Hassan S. Al-Basha, Ph.D.

McMaster Nuclear Reactor
McMaster University
Hamilton, Ontario L8S 4K1

SUMMARY

This paper presents the results of the reactor physics analysis performed to support the conversion of the McMaster Nuclear Reactor (MNR) from the use of HEU fuel to LEU fuel. The overall objective of this work was to demonstrate that the use of LEU fuel will not change the present performance or safety margins of the MNR core. The LEU silicide fuel that will be used in the MNR has been approved by the US Nuclear Regulatory Commission (USNRC) for use in non-power reactors. The new LEU assemblies have the same overall design as the current HEU assemblies with the exception of the fuel composition.

The methods and codes used in this work have been qualified by AECL [1] and MNR [2] for use in this type of analysis. The reactor parameters investigated in this work were those that could change as a result of using LEU fuel in the core instead of HEU fuel. The results show that MNR facility can be operated as safely with the new LEU fuel as with the present HEU fuel. There is no significant change to the operating safety margin of the MNR as a result of using LEU fuel.

It is worth noting that since 1988, the MNR core has operated with two LEU fuel assemblies at two low power core positions. The AECB approved the use of these two assemblies in 1988. They are identical in overall design and enrichment to the new LEU fuel assemblies which MNR plans to use later this year. The only difference is the new LEU assemblies have a lower ^{235}U loading (225 grams vs. 284 grams) which is more conservative in terms of assembly power peaking factors and reactivity. The new LEU fuel assemblies have nearly the same power peaking factors as the current 18-plate HEU assemblies.

1.0 Introduction

This paper describes the analysis methods and results of the reactor physics calculations performed to support the use of LEU fuel in the MNR core in place of HEU fuel. The objective of this work is to show that the use of LEU fuel will not compromise the operating safety margin of the MNR with regard to shutdown margin and assembly peaking power. The new LEU fuel assembly has the same overall design as the present HEU fuel assembly, except for fuel composition. The new standard LEU fuel assembly contains 225 grams of ^{235}U in 19.75% enriched U_3Si_2-Al fuel, whereas the present standard HEU fuel assembly contains 196 grams of ^{235}U in 93% enriched U-Al alloy fuel. The LEU control assembly contains 112.5 grams of ^{235}U in 19.75% enriched U_3Si_2-Al fuel, while the HEU control assembly contains 110 grams of ^{235}U in 93% enriched U-Al alloy fuel.

The MNR core is a heterogeneous, light water moderated and cooled, swimming-pool type reactor fuelled with 93% enriched MTR-type U-Al alloy fuel. The total loading of a typical operating MNR core is about 4.6 kg of ^{235}U . The reactor is controlled by means of five shim rods and one regulating rod. The shim rods are Ag (5 w%)-In (10 w%)-Cd (85 w%); the regulating rod is stainless steel. The oval control rod is surrounded by fuel plates; four fuelled plates on one side and five fuelled plates on the other side.

The reference core analyzed in this work is core 48A which consisted of 20 18-plate HEU fuel assemblies, eight 10-plate HEU fuel assemblies, two 18-plate LEU fuel assemblies, and six 9-plate HEU control assemblies. The complete LEU reference core used in this analysis is the same as core 48A with all fuel assemblies (28 HEU, 2 LEU-old, and 6 control) replaced by new LEU fuel assemblies with equivalent exposure (MWD's). A mixed HEU-LEU core was also investigated in this work. This core was similar to core 48A, except that 10 standard and 3 control HEU assemblies were replaced with LEU assemblies of the same type with equivalent exposure (MWD's). This core was investigated because the conversion to complete LEU core is expected to be carried out over several years. The LEU fuel assemblies will be placed in the core either as needed in terms of overall core excess reactivity for continued operation or as HEU fuel assemblies are removed from the core. The core excess reactivity at all times will be limited by the criteria approved by the AECB in the current MNR operating license and SAR. The LEU core (mixed or complete) will use the same control system, heat removal system and auxiliary systems as the current HEU core.

2.0 Fuel Assembly Descriptions

The external and internal dimensions of the 18-plate HEU and LEU fuel assemblies are identical. Figure 2.1 shows a schematic of a typical 18-plate MNR fuel assembly along with relevant information such as geometries, material and fissile loading of the two assemblies. Both are manufactured by CERCA of France and the only difference between the two is the fuel composition.

3.0 Calculational Models

3.1 Nuclear Cross-Sections for Diffusion Theory Models

WIMS-AECL was used to generate cell averaged cross-sections for the various regions in the MNR core. Figure 3.1 shows the core configuration with burnup information for core 48A. In this core there are three types of fuel assemblies: 20 18-plate HEU assemblies, 8 10-plate HEU assemblies, and 2 18-plate LEU assemblies. The core is reflected by graphite on the south side, lead and water on the west side, and only water on north and east sides.

3.1.1 Standard Fuel WIMS-AECL Models

Several WIMS-AECL models were developed to represent all types of fuel assemblies present in the core and the new replacement LEU assemblies. The 1D infinite-slab option in WIMS-AECL was used with the model preserving the volume fraction of each of the fuel, clad, and water. The WIMS-AECL models used consisted of only modelling half of the assembly because of symmetry. For example, the 18-plate assembly was modelled using 8 fuelled plates and one non-fuelled plate (dummy). Two extra regions were added beyond the ninth plate, the first region accounted for aluminum in the two side plates and in the non-fuelled regions of the assembly and the second region was used to represent the extra water present in the non-active portion of the fuel assembly and that between adjacent assemblies. Similar WIMS-AECL models were used for both the HEU (18-plate) and LEU assemblies with the only difference being the fuel composition. Similar arrangement was used to model the 10-plate HEU fuel assemblies. The external dimensions of the 10-plate assemblies are nearly identical in shape and size to the 18-plate assemblies except no dummy plates are used and all ten plates contain fuel.

In all the fuel models the actual thickness of the fuel, clad, and water gap were used. For example, in the case of the 18-plate assembly (both HEU and LEU), the active fuel thickness was 0.0508 cm, the cladding thickness on each side of active fuel was 0.038 cm, and the water gap between adjacent fuel plates was 0.30 cm. In the case of a 10-plate fuel assembly, the active fuel thickness was 0.0508 cm, the cladding thickness on each side of active fuel was 0.0508 cm, and the water gap between adjacent plates was 0.635 cm.

Two additional WIMS-AECL models were developed to represent the non-active top and bottom portions of the fuel plates. One model was for the 18-plate assembly (both HEU and LEU assemblies), and the second one was for the 10-plate assembly. In both of these models the fuel meat was replaced by aluminum in the active region of the plates.

There are six 9-plate control assemblies in the core; one with a stainless steel absorber (regulating) rod and the rest with Ag/In/Cd absorber rods. Two sets of WIMS-AECL models, each consisting of four models, were developed for the control assemblies; one for HEU control assemblies and the other for LEU control assemblies. In each set, two models were used for the shim rods and the other two for the regulating rod. One model represented a fully inserted absorber and the other was for a fully withdrawn absorber. When the rod is fully inserted the absorber material is included in the model, whereas water was used to represent a fully withdrawn rod.

WIMS-AECL models were also developed to represent the graphite blocks, lead shield, and the beryllium block. The cross-sections for these regions were generated using the select option in WIMS-AECL. This option extracts region-averaged cross-sections from the region-of-interest in the WIMS-AECL calculation. The select model consisted of a quasi-fuel region, a water gap, and the region-of-interest. The elements in the region-of-interest varied depending on the material and the region being modelled. The size of the region-of-interest was proportional to the region being modelled, and the size of the water gap between the quasi fuel region and the region-of-interest was chosen to represent the actual spacing between the region-of-interest and the nearest fuel assembly.

The cross-sections for the water reflector and central irradiation facility were generated using a homogeneous unit cell model with appropriate number density for all the elements in the region of interest. A very small concentration of ^{235}U (10^{-10} atom/b-cm) was added to the unit cell to generate the necessary neutron spectrum in the cell. The "homogeneous" cell option in WIMS-AECL was used in these models. The use of the homogeneous cell option of WIMS-AECL for this type of analysis was recommended by ANL. [3].

The region 15 centimeters above and below the active core was modelled using one WIMS-AECL model with the homogeneous cell option. The material composition for this region was assumed to consist of 80 v% water and 20 v% aluminum. This was done to reduce the complexity of the calculations in the axial direction.

The WIMS-AECL calculations were performed using the library's full energy structure; 89-groups for non-fuelled core regions and 34-groups for fuelled core regions. The region-averaged or cell-homogenized cross-sections in the binary output files (89-groups or 34-groups) of WIMS-AECL were collapsed to the 7-group energy structure discussed in Reference 2 using the code CONDENS-AECL. Table 3.1 shows the 34-group neutron energy structures that were used in the WIMS-AECL calculations for the fuelled region and the 7-group energy structure used in the global 3-D diffusion calculations. The 7-group energy structure used in this work is similar to the one used by ANL for the conversion of the Georgia Tech Research Reactor (GTRR) from HEU to LEU fuel [4].

3.2 Three-Dimensional Diffusion Model

The computer code, 3DDT, was used to perform detailed three-dimensional diffusion calculations for MNR. The diffusion cross-sections for the various regions in the core were generated using WIMS-AECL. The X-Y reactor model of the MNR core is shown in Figure 3.2. In each fuel or control assembly on average 6 x-meshes and 6 y-meshes were used for an average radial mesh size of 1.35 cm x 1.285 cm. There were 42-x meshes (row 1-7) and 43-y meshes (row A-F) in the active core region. The graphite blocks, the beryllium block, and the water reflector inside the grid plate (zones 1A, 1B, and 7A, 5C, 9A, etc.) were also modelled using a 6-x and 6-y mesh scheme. There were 12 x-meshes and 5 y-meshes in the lead region. The core was surrounded by pool water on all sides; 15 cm on the South side, 20 cm on the North side, 10 cm on the East side, and 7 cm on the West side beyond the lead shield.

The active height of the fuel region was 60 centimeters, however, only 30 centimeters were modelled because axial symmetry was assumed. In the active core region 10 axial-meshes (10@3.0 cm) were used. Two regions were modelled above the active core, the first region was 15 cm (6 meshes @ 2.5 cm) long and consisted of 80 v% water and 20 v% aluminum, whereas the second region was 5 cm long (2 meshes @ 2.5 cm) and consisted of water only. This axial model approximation was used to simplify the axial description of the reactor, and it does not considerably change the accuracy of the results. The difference between this model and the detailed one used in Reference 5 is discussed in section 4.5. The beam ports in the reactor were not modelled in this work to simplify the core model, and because diffusion theory is not valid in voided regions. The impact of these model simplifications on the results is discussed in section 4.5.

3.3 Reactor Physics Calculations for MNR

Reactor physics calculations were performed to investigate any possible changes to the operating safety margin of the MNR as a result of converting the reactor from the use of HEU fuel to LEU fuel. Critical core parameters such as the flux and power distributions, total power peaking factors, control rods reactivity worth, and isothermal reactivity feedback were calculated for three different cores. The reference core used in this work was core 48A which is a typical operating core; a complete LEU core (48A-LEU) and a mixed HEU-LEU (48A-MIX) core were also used in this work. The mixed HEU-LEU core was obtained by replacing 10 standard and 3 control HEU assemblies with LEU fuel assemblies of the same type (10 standard and 3 control). The exposure in MWD's of all the fuel assemblies in all three cores was the same. Table 3.2 shows the core positions and exposures for the 13 HEU fuel assemblies removed from core 48A and their LEU replacement. Fuel depletion calculations were performed using WIMS-AECL for all types of fuel assemblies present in core 48A and the new LEU fuel assemblies.

The reactivity worth of each control rod was determined by comparing the calculated core reactivity with the rod fully inserted and fully withdrawn. The reactivity worth for the all safety rods was determined for the reference core (core 48A), and the HEU-LEU mixed core and the complete LEU mixed core.

Calculations were also performed for the three cores to estimate the isothermal reactivity coefficients for change of water temperature only, change of water density only, and change of fuel temperature only. In the change of water temperature only calculations, the temperature of the water in the active core region was changed to 50 °C and 100 °C with the water density kept constant at 0.9984 g/cm^3 (20°C). In the case of change of water density only, the calculations were performed for water density of 0.988 g/cm^3 (50 °C), 0.958 g/cm^3 (100 °C), and 0.8 g/cm^3 with the water temperature kept constant at 20 °C. An additional case was performed with the water density at 0.80 g/cm^3 and with water temperature at 100 °C. The fuel and clad temperatures in these calculations were kept constant at 20 °C. K_{eff} was computed for each case using 3DDT and the reactivity feedback coefficients were determined for each feedback mechanism. The fuel Doppler effect was also determined by changing only the fuel temperature from 20 °C to 100 °C and 200 °C . The change of reactivity was determined by comparing the computed K_{eff} for each case. The reference case in this work was assumed to be with the temperature of the fuel, clad, and water at 20 °C, and the operating case with the temperature of the fuel, clad, and water at 46 °C, 45 °C, and 36.5 °C, respectively.

4.0 Results and Discussion

Reactor physics calculations were performed to investigate the conversion of the MNR from the use of HEU fuel to LEU fuel. Critical core parameters such as power peaking factors, safety rods worth, and isothermal reactivity feedback were determined for the three cores analyzed in this work. Xenon worth was determined for a typical HEU and LEU cores. Model validation for operating cores 48A, 48B, 48C, 48D, and 48K was also performed to determine accuracy and reliability of the calculations. This was accomplished by comparing the excess reactivity for each core with measured data, and by comparing the change in reactivity for each core change (i.e. core 48A to 48B, core 48B to 48C, core 48C to 48D, and core 48J to 48K) with measured values.

4.1 Neutron Flux and Power Distributions

The neutron flux and power distributions were determined for core 48A, 48A-LEU, and 48A-MIX. The neutron flux profiles along row C for the three cores are shown in Figure 4.1 for three energy groups ($E \geq 821$ keV, $0.625 \text{ eV} < E < 821$ keV, $E \leq 0.625$ eV). The calculated thermal flux for the central irradiation facility (5C) for $E \leq 0.625$ eV is 5.3×10^{13} n/cm^2 s for core 48A, and 5.2×10^{13} n/cm^2 s and 5.0×10^{13} n/cm^2 s for the mixed HEU-LEU and the complete LEU cores, respectively. The thermal flux decreased by 6% for the complete LEU core, which is expected due to the increase in absorption in LEU fuel because of the larger ^{235}U loading.

The measured thermal flux for a typical HEU core is in the range of 4.4×10^{13} n/cm^2 s to 4.6×10^{13} n/cm^2 s. The measured value for the thermal flux was obtained using a self powered neutron detector (SPND). The difference between the two results is larger than expected but is within the uncertainty of the calculational technique and the uncertainty associated with the cut-off thermal energy boundary for the SPND. Validation calculations using the IAEA benchmark problem (10 MW benchmark reactor) showed that the 3DDT calculated thermal neutron flux for the central trap is nearly identical to that calculated by ANL [2]. This only shows that the calculational methodology used in this work yields similar results to that of other international laboratories such as ANL, it does not, however, give any information about the accuracy of the results presented here. Only comparison with measured data would provide the information needed to determine the accuracy of the methodology used in this work.

The 3DDT calculated assembly power for the three cores are shown in Figure 4.2. As seen from this figure, the largest assembly power was for core position 3D for all three cores. The assembly in this position had a very low exposure (low burnup), and thus contained the highest amount of fissile material. It is important to note that the assembly powers for the three cores are very similar, with the largest difference between core 48A and 48A-LEU. The results in Figure 4.2 show that for most of the core regions the assembly powers in the LEU core were only slightly different than in core 48A. This was most noticeable for assemblies with high burnup. This is because the burnup rate for LEU fuel is slightly smaller than for HEU fuel, which means for the same exposure LEU fuel assemblies would have slightly more fissile material. This of course assumes that the increase in ^{235}U loading in LEU fuel assemblies is just to compensate for the increase in the parasitic neutron absorption of ^{238}U.

The total power peaking factors for several core positions were compared for the three cores. In this work, the total power peaking factor is defined as the product of a radial peaking factor and a local peaking factor. The radial power peaking factor is defined as the ratio of the average midplane power in a fuel bundle to the average midplane power in all fuel assemblies in the core. The local power peaking factor is defined as the ratio of the maximum midplane power to the average midplane power in a specific assembly. Adequate radial mesh points were used for each fuel assembly (6 x and 6 y) so that reasonable local power peaking factors can be obtained. The total power peaking factors were calculated for core positions 3D, 4C, and 4D for the three cores, as shown in Table 4.1. The maximum difference occurred for the mixed HEU-LEU core. This is because of the several different types of fuel assemblies present in the core. However, the peaking factors for the mixed core are within those measured for various MNR cores. This indicates that using LEU fuel with higher ^{235}U loading than current HEU fuel will not compromise the power peaking safety limit for the MNR.

4.2 Control Rod Reactivity worth

The next set of calculations were performed to determine the reactivity worth of the shim rods and the regulating rod for all three cores. The reactivity worth of the safety rods were measured after core 48A was configured on or about May 12, 1996. The absorber material, which is Ag/In/Cd for the shim rods and stainless steel for the regulating rod, was homogenized over the fuel assembly. This approach will slightly under-predict the reactivity worth of the shim rods because the absorber material is being homogenized over a large region. This will reduce its effective absorption cross-sections.

The reactivity worth for each rod was determined by calculating the change in reactivity as the safety rod is completely inserted into the core. The rod was assumed to have a height of 62.55 cm. The absorber and its aluminum cladding were replaced by water in the calculations when the rod was assumed to be completely withdrawn. Table 4.2 shows the calculated and measured (only for core 48A) reactivity worth for the shim and regulating rods for all three cores. The calculated reactivity worth for the regulating rod for core 48A was nearly identical to the measured one. In the case of the shim rods, the calculated reactivity worth was less by 2-4 mk , except for shim rod # 1 where the calculated worth is higher by about 2 mk. Two factors that may have contributed to the difference between calculated and measured reactivity worth for the shim rods for the HEU core. This includes the approach used to model the absorber material and the accuracy of the burn-up data used in the calculations. The calculated total worth of the safety rods for the mixed HEU-LEU core was slightly less than that of core 48A, and it was 7% less for the complete LEU core. The small reduction in the total worth of the safety rods for the complete LEU core will not impact the shutdown margin of the MNR. This is because during each core refuelling a test will be performed to ensure that the newly refuelled core meets the shutdown margin requirements. The reduction in the shim rods worth will only impact the available core operating excess reactivity, which means a lower available core excess reactivity for continued operation. Further, the worth of the shim rods for the LEU core can be increased by replacing the control assemblies more frequently (i.e. lower exit burnup) or by moving them into higher flux positions. This will increase the thermal flux in the control assemblies, and hence the worth of the shim rods.

4.3 Isothermal Reactivity Feedback

4.3.1 Change of Water Temperature Only and Water Density Only

The effective multiplication factor, k_{eff}, was calculated for cores 48A, core 48A-LEU, core 48A-MIX as a function of change of water temperature only and a change of water density only. WIMS-AECL was used to generate cell-averaged cross-sections for each fuel assembly type. Table 4.3 shows k_{eff} and the reactivity changes relative to the reference case of 20°C, the typical range of the water temperature during normal operation is around 36.5 °C averaged axially. As expected the increase in water temperature reduced the reactivity for core 48A, and the reduction in reactivity was less for the mixed and complete LEU cores. The reduction in core reactivity as a function of increased water temperature is due to the slight reduction in the moderating power of hydrogen atoms as the water temperature is increased. This results in a slightly harder neutron spectrum in the core, and the feedback effects are slightly less negative for the LEU fuel than for HEU fuel. The values reported in Table 4.3 underpredict the actual effects of increased water temperature because the water temperature outside the active core region was kept constant at 20 °C. This will reduce the overall neutron leakage (axial and radial) from the core, and when this factor is included in the analysis, the real effect of increased water temperature will be larger depending on the temperature of the water outside the active core region.

Similar results were also obtained for the change of water density only. The reduction in the density of the coolant in the active core region reduced the reactivity of the core because of a decrease in core moderation. This effect was the largest for the complete LEU as can be seen from Table 4.4. This is because the neutron spectrum in the LEU core is slightly harder than that of the HEU core, and any reduction in moderation would considerably increase the resonance absorption of epithermal neutrons in the LEU fuel. The use of LEU fuel in this case will not compromise any safety feedback from the change in water temperature and density. Although, the reactivity feedback from a change in water temperature is less for the LEU fuel than for HEU fuel, it is well compensated for by the additional margin form the change of water density, thus, the net effect is in favor of the LEU fuel. This can be seen from the last case in Table 4.4 where both the water temperature and density were changed to simulate a 20% voiding of the coolant in the active core. The result is slightly more conservative for the LEU core.

4.3.2 Change of Fuel Temperature Only

Core calculations were performed for several fuel temperatures to determine the core multiplication factor as a function of fuel temperature. Cell-averaged cross-sections were generated for each type of fuel assembly in the core for fuel temperatures of 100 °C and 200 C. The cell-averaged cross-sections for each case was then used in 3DDT to determine k_{eff}. Table 4.5 presents the calculated k_{eff} and reactivity changes relative to the 20 °C reference case. It can be seen from this table that the Doppler effect for the HEU case is relatively small. This is because the effect of fuel temperature changes is entirely a resonance absorption effect in ^{238}U, which is at low concentration in HEU fuel. This effect is larger for the complete LEU core because of its considerably larger ^{238}U loading. Thus, the use of LEU fuel will provide a larger safety margin for containing any unforeseen power increases. The net effect of change of the fuel/water temperatures and water density is more conservative for the LEU fuel for both complete LEU and mixed HEU-LEU cores.

4.4 Xenon Reactivity Worth

WIMS-AECL calculations were performed for all types of fuel assemblies currently present in the core and for the new LEU fuel assembly to determine the global reactivity worth of xenon in an HEU core and a complete LEU core. One set of WIMS-AECL cross-sections was with xenon concentration at the various assembly burnup conditions and another set was with xenon concentrations set to zero. These two sets were used in 3DDT to determine the global xenon effect. The core calculations were performed for a typical HEU core and for a complete LEU core. Table 4.6 shows the 3DDT calculated K_{eff} for the two cores with and without xenon present in the core. As seen from this table, the xenon reactivity worth for the HEU core is nearly identical to the LEU core. The LEU fuel has higher ^{235}U loading, which will reduce the thermal flux in the core because of increased absorption. Thus, the concentration of xenon will slightly increase in the LEU core because less xenon is being burned in the core. However, because of the lower thermal flux in the core, less ^{135}I is being produced in the LEU core which means less xenon is being produced from the decay of iodine. These two effects cancel each other and, thus, the xenon worth for the LEU core is nearly the same as for the HEU core.

4.5 Model Validation and Sensitivity Analysis

The core model used in the present work was validated by comparing the calculated change in core reactivity and the core excess reactivity for several cores with measured values. The core changes simulated in this analysis are: 48A to 48B; 48B to 48C; 48C to 48D; 48J to 48K. Also, when core 48A was configured the reactivity worth of a highly irradiated assembly (39 %BU) in an empty core position (7A) was measured. This experiment was simulated using fuel element MNR-220 which on May 12, 1996 had a 39 %BU. Table 4.7 shows the calculated core excess reactivity after the core change and the change in reactivity as a result of the core change for the four core changes.

The calculated core excess reactivity for all core changes is within 10 mk of measured values, which is reasonable considering the various modelling approximations used in this work and the uncertainty associated with the measured values. It is interesting to note that for several core changes the difference was much less than 10 mk. The calculated change in core reactivity as a function of the refuelling operation is within 1 mk of the measured values, which is extremely good considering again all the approximations made in this work including the uncertainty associated with assembly burnup and cross-sections. The calculated reactivity worth of the fuel element MNR-220 in the empty core position 7A is again within 1 mk of the measured value. This shows that the models and tools used in this work are reliable and reasonably accurate for reactor lattice calculations for research reactors using HEU MTR-type fuel such as the MNR. The results and conclusions presented here are not expected to change for the mixed or complete LEU cores.

The model used in this work was simplified from the model discussed in Reference 5. There were two simplifications including the removal of the beam ports from the model and using only two regions above and below the active core region. The beam ports were removed from the core model since diffusion theory is not valid in voided regions such as the beam ports. The calculated k_{eff} for the simplified model was reduced by the measured worth of the beam ports which is 3 mk. This value is reported in the SAR for an experiment conducted in 1972 where all the beam ports were flooded. The calculated value for the beam ports based on the model in Reference 5 was 5.5 mk.

The second simplification is for the regions above and below the active core zone. The model used in Reference 5 contained five regions below the active fuel and two regions above the active fuel. The regions below the active fuel were for the assembly bottom end regions, while the regions above the active fuel were for the assembly top end box and the water above the assembly. In similar calculations, ANL normally uses a two region approach with the first region being 80 v% water and 20 v% aluminum to represent the top and bottom sections of the core followed by a second region of water only. Similar, arrangement was used in this work, with the first region being 15 cm long and the second region 5 cm long. The second region was only 5 cm long because of computer memory limitation due to the fine spatial mesh scheme used in this work. The difference between this model and the one used in Reference 5 was found to be less than 2 mk.

5.0 Conclusions

The results presented in this paper show that using LEU fuel in the MNR will not reduce any of the reactor operating safety margins, and that the reactor can be operated as safely with the new LEU fuel as with the present HEU fuel. The LEU fuel analyzed in this work has more negative reactivity feedback for change of water density only and change of fuel temperature only, and slightly less for change of water temperature only than currently used HEU fuel. However, the combined effects of all three feedback mechanisms is more negative for the LEU fuel than HEU fuel. The change to LEU fuel will slightly reduce the total worth of the safety rods in the core. This will only reduce available core excess reactivity for continued operation, and will not compromise the reactor shut-down margin requirement.

6. References

[1] R. J. Ellis et al, *A Validation of the WIMS-AECL/3DDT Against SPERT-1B Reactivity Measurements*. AECL-WL Technical Note, RTB-TN-017, April 1994.

[2] H. S. Basha, *Validation of WIMS-AECL/3DDT Code Package for MNR Fuel Conversion Analysis Using The IAEA 10 MW Benchmark Reactor*, MNR Technical Paper, April 1998.

[3] Jim Deen, ANL, Private Communication with H. S. Al-Basha, February 1998.

[4] J.E. Matos, S.C., and W.L. Woodruff, *Analyses for Conversion of the Georgia Tech Research Reactor from HEU to LEU*, ANL, RERTR Program, September 1992.

[5] H. S. Basha, *Reactor Physics Simulation of the MNR HEU Core*, MNR Technical Paper, MNR-TR-97-05, July 1997.

[6] *MNR Safety Analysis Paper*, 1972.

[7] *Research Reactor Core Conversion from the Use of HEU to the USE LEU Guidebook*. IAEA Paper, IAEA-TECDOC-233, 1980.

TABLE 3.1 Neutron Energy-Group Structures Used in WMIS-AECL and 3DDT Calculations.

	Lower Limit (eV)	
Group	WIMS-AECL	3DDT
1	3.68×10^{6}	
2	1.35×10^{6}	
3	8.21×10^{5}	8.21×10^{5}
4	4.98×10^{5}	
5	4.09×10^{4}	
6	9.12×10^{3}	9.12×10^{3}
7	5.53×10^{3}	
8	1.30×10^{2}	
9	4.78×10^{1}	
10	1.37×10^{1}	
11	1.07×10^{1}	
12	4.0000	
13	3.3000	
14	2.6000	
15	2.1000	2.1000
16	1.3000	
17	1.1500	1.1500
18	1.1000	
19	1.0200	
20	0.9700	
21	0.9500	
22	0.8500	
23	0.6250	0.6250
24	0.4000	
25	0.3200	
26	0.2500	
27	0.1800	
28	0.1400	0.1400
29	0.1000	
30	0.0800	
31	0.0500	
32	0.0300	
33	0.0150	
34	0.0002	0.0002

Table 3.2 The Fuel Assemblies in Core 48A that were Changed to LEU in Core 48A-MIX Along with their Core Positions and Exposure in MWDs.

Core Position[1]	Fuel Assembly	Exposure (MWh)
2E[2]	CI116-S	0
3B	MNR-180	1498
3C	MNR-186	1480
3D	CI-618	157
4A	CI-612	680
4B[2]	MNR-C44	301
4C	MNR-184	1448
4E[2]	CI115-S	190
5B	MNR-227	1176
5D	MNR-225	1348
5E	MNR-183	1453
6C	MNR-220	1452
6D	CI-616	493

1. See Figure 3.1.
2. Control assembly.

Table 4.1 The Total Power Peaking Factors for Several Core Positions in Core 48A, 48A-MIX, and 48A-LEU.

Core Position	48-A	48A-MIX	48A-LEU
3D	1.87	1.94	1.68
4C	1.71	1.94	1.88
4D	1.61	1.50	1.76

Table 4.2 Comparison of 3DDT Calculated Reactivity Worth for the MNR Safety Rods for Core 48A, 48A-MIX, 48A-LEU

Safety Rod #	Reactivity Worth (mk)			
	48A[1]	48A[2]	48A-MIX[2]	48A-LEU[2]
Regulating	3.94	4.07	3.85	3.65
Shim # 1	13.90	16.20	15.31	15.85
Shim # 2	17.50	15.35	13.82	14.30
Shim # 3	22.70	18.65	18.77	17.90
Shim # 4	13.10	10.67	10.70	9.61
Shim # 5	25.10	24.33	22.85	21.95
Total	92.30	85.20	81.48	79.61

1. Measured on May 12, 1996
2. Calculated using WIMS-AECL/3DDT

Table 4.3 Reactivity Effects For Change of Water Temperature Only for Core 48A, 48A-MIX, and 48A-LEU.

T (^{0}C)	k_{eff} ($\Delta\rho$(mk))		
	48A	48A-MIX	48A-LEU
20[1]	1.0148 (0.0)	1.0289 (0.0)	1.0382 (0.0)
50	1.0135 (-1.23)	1.0259 (-0.91)	1.0376 (-0.48)
100	1.0108 (-3.88)	1.0238 (-2.95)	1.0362 (-1.85)

1. Reference case with all regions at 20 ^{0}C

Table 4.4 Reactivity Effects For Change of Water Density Only for Core 48A, 48A-MIX, and 48A-LEU.

Density	k_{eff} ($\Delta\rho$(mk))		
(g/cm^3)	48A	48A-MIX	48A-LEU
0.9984[1]	1.0148 (0.0)	1.0289 (0.0)	1.0382 (0.0)
0.9880	1.0137 (-1.04)	1.0257 (-1.14)	1.0367 (-1.36)
0.9580	1.0100 (-4.59)	1.0216 (-5.11)	1.0321 (-5.67)
0.8000	0.9863 (-28.50)	0.9956 (-30.56)	1.0034 (-33.33)
0.8000[2]	0.9730 (-42.30)	0.9838 (-42.67)	0.9925 (-44.30)

1. Reference case with all regions at 20 ^{0}C
2. Water temperature is changed to 100 ^{0}C from 20 ^{0}C

Table 4.5 Reactivity Effects For Change of Fuel Temperature for Core 48A, 48A-MIX, and 48A-LEU.

T (^oC)	$k^1_{eff}(\rho, mk)$		
	48A	48A-MIX	48A-LEU
20[1]	1.0148 (0.0)	1.0289 (0.0)	1.0382 (-0.0)
100	1.0146 (-0.16)	1.0263 (-0.60)	1.0371 (-0.90)
200	1.0143 (-0.49)	1.0255 (-1.36)	1.0359 (-2.11)

1. Reference case with all regions at 20 ^0C

Table 4.6 Xenon Reactivity Worth for Core 48A and 48A-LEU.

Core	$\Delta\rho$(mk)	k_{eff}(Xe)	k_{eff}(no Xe)
48A	-21.7	0.99461	1.01657
48A-LEU	-21.4	1.0084	1.03067

Table 4.7 Comparison of Calculated and Measured Core Excess Reactivity for Several MNR Core Changes.

Core (Date)	$\rho_{excess}(\Delta\rho, mk)$	
	Calculated	Measured
48A(5/12/96)	37.0 (6.4)	33.0 (6.0)
48B(8/18/96)	39.5 (12)	33.4 (10.7)
48C(11/24/96)	34.8 (6.6)	27.9 (5.9)
48D (1/19/97)	32.4 (1.8)	27.1 (2.3)
48K(1/25/98)	34.1 (3.4)	23.3 (3.0)
48A-MNR220-7A	(3.7)	(3.3)

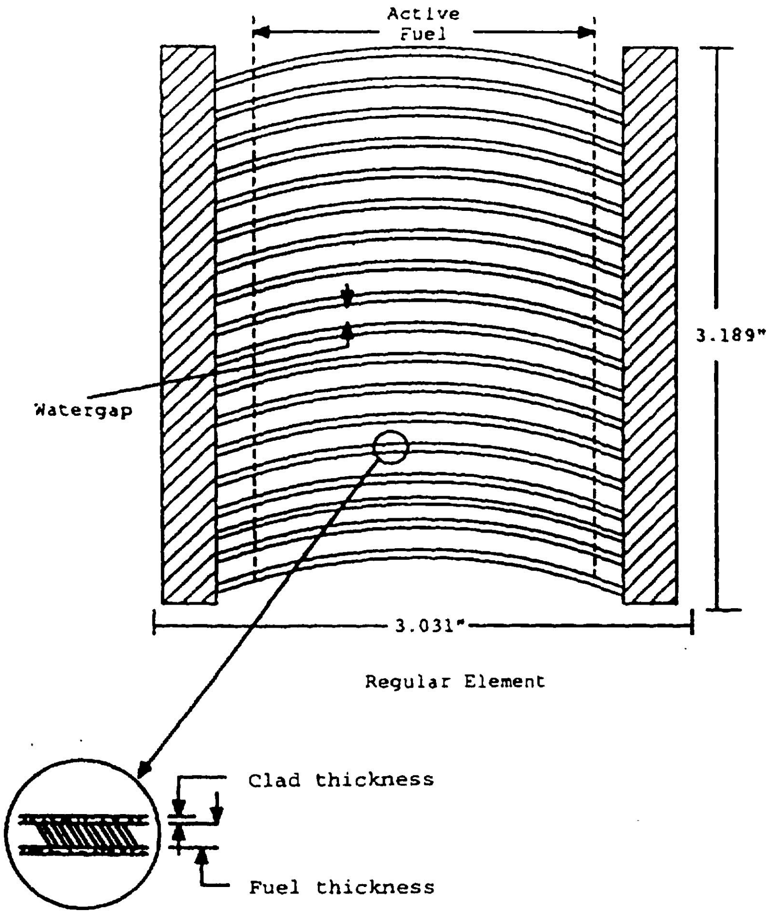

	HEU	LEU
Number of Fueled Plates/Assembly	16	16
Number of Non-Fueled Plates/Assembly	2	2
Enrichment, w%	93	19.75
Fissile Loading/Plate, g 235U	196	225
Fuel Meat Composition	U-Al Alloy	U_3Si_2-Al
Cladding Material	Al	Al
Fuel Meat Thickness, mm	0.508	0.508
Cladding Thickness, mm	0.38	0.38
Water Gap Thickness, mm	3.0	3.0

Figure 2.1 A Schematic of a Typical Fuel Bundle for the MNR Along with Relevant Information.

9	8	7	6	5	4	3	2	1	
W	G	W	MNR302 24%	CI617 11%	CI612 19%	PTR38 30%	Be	W	A
W	G	CI613 15%	MNRC57 25%	MNR227 33%	MNRC44 15%	MNR180 42%	MNR223 41%	W	B
W	G	PTR52 18%	MNR220 40%	W	MNR184 41%	MNR186 42%	CI105S 10%	PTR49 22%	C
G	G	PTR62 245	CI616 14%	MNR225 375	PTR58 26%	CI618 5%	PTR44 38%	CI615 125	D
W	G	MNR200 42%	CI114S 0%	MNR183 41%	CI115S 10%	MNR188 42%	CI116S 0%	CI614 12%	E
W	G	G	PTR61 17%	MNR218 33%	MNR301 29%	CI603 15%	PTR53 24%	MNR215 49%	F

N

PTR 10-Plate HEU Fuel
MNRC57, MNRC44, CI115S, CI116S, CI105S Control Elements with Shim Rods
CI114S Control Element with Reg. Rod
MNR301 @ MNR302 18-Plate LEU

Figure 3.1 Fuel Map and Burn-up Data for Core 48A.

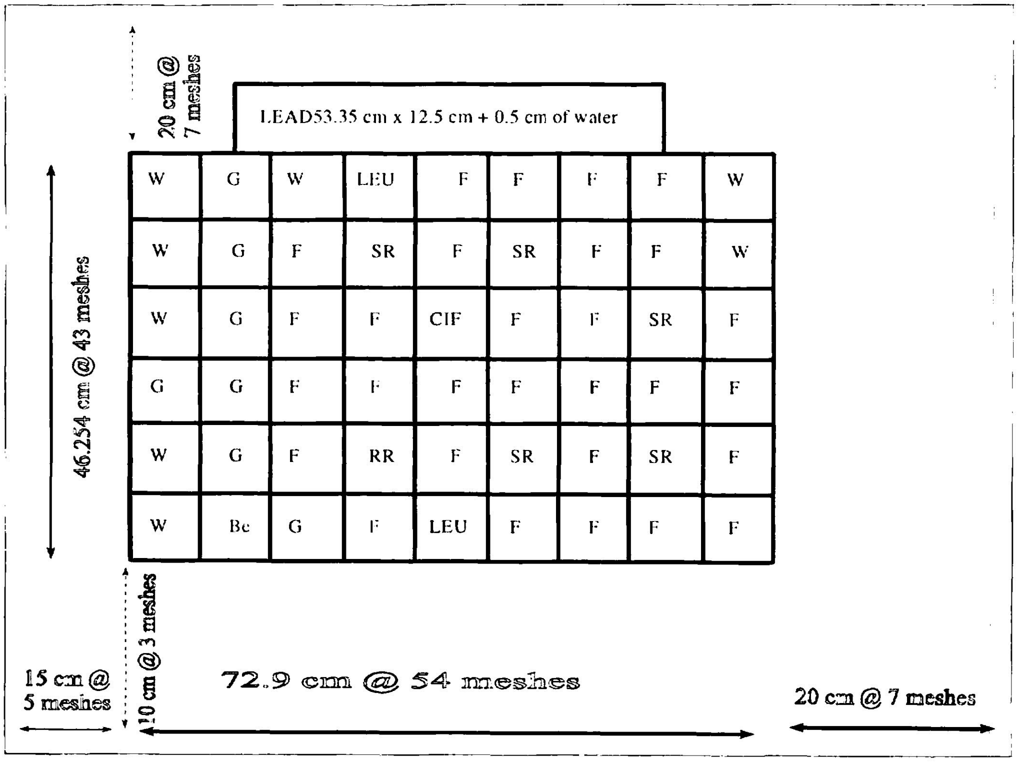

Figure 3.2 The 3DDT X-Y Core Model for the MNR.

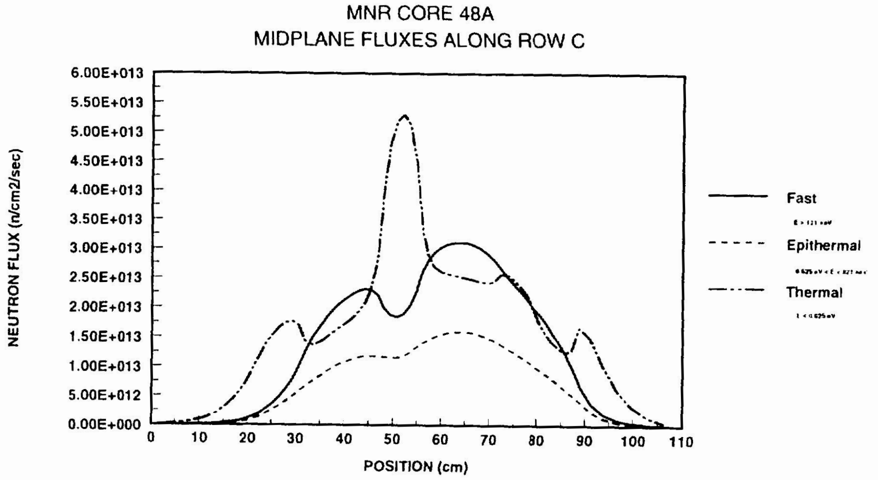

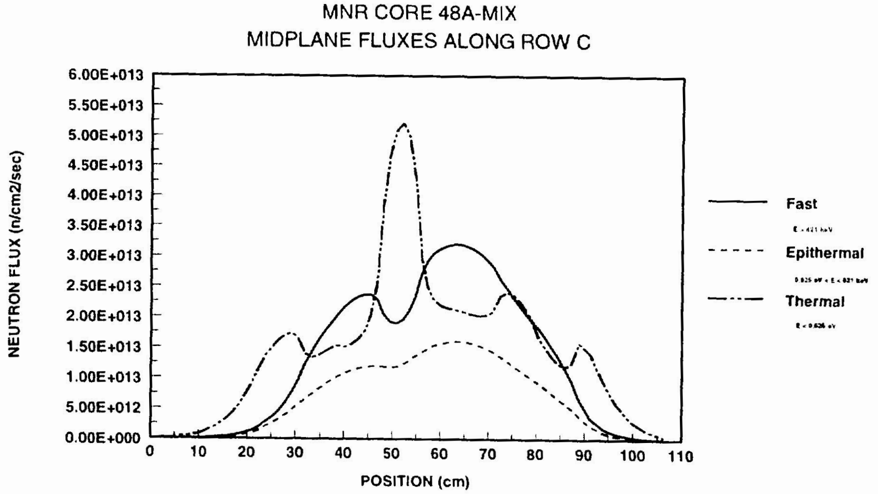

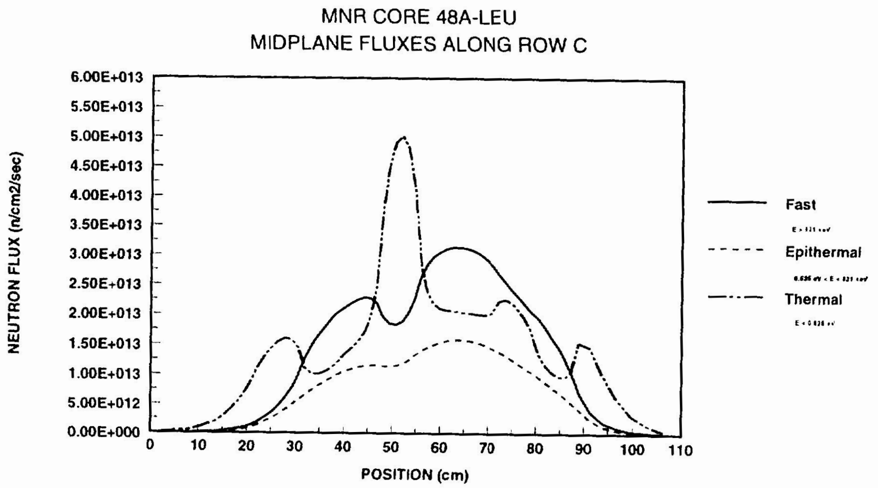

Figure 4.1 The Radial Distributions of the 3DDT Calculated Neutron Fluxes through Row C at Core Mid-Plane Axial Position for Cores 48A, 48A-Mix, and 48A-LEU.

	7	6	5	4	3	2	1
A		MNR302** 49.3 48.7 39.7	CI617 50.5 49.0 50.0	CI612* 53.4 56.3 53.3	PTR38 45.6 44.2 50.1		**Element** **(48A)** **(48-MIX)** **(48A-LEU)**
B	CI613 46.6 45.9 45.6	MNRC57 35.5 34.1 33.7	MNR227* 66.8 72.8 69.8	MNRC44* 50.2 51.9 47.5	MNR180* 58.2 63.8 61.6	MNR223 50.9 48.9 55.5	
C	PTR52 48.2 47.1 48.6	MNR220* 59.4 65.3 61.8		MNR184* 77.4 85.5 82.0	MNR186* 67.7 73.3 72.3	CI105S 48.9 46.5 45.1	PTR49 46.5 44.3 50.9
D	PTR62 46.7 45.5 48.4	CI616* 70.1 71.3 67.9	MNR225* 75.2 81.1 77.2	PTR58 83.1 79.0 87.1	CI618* 95.9 95.9 89.9	PTR44 60.7 57.5 68.0	CI615 53.8 50.7 52.2
E	MNR200 37.6 36.9 39.8	CI114S 45.3 43.2 40.8	MNR183* 61.0 66.6 63.8	CI115S* 56.4 58.0 51.6	MNR188 63.9 60.3 67.1	CI116S* 50.4 50.5 44.7	CI614 48.8 45.3 48.2
F		PTR61 46.0 44.7 47.6	MNR218 49.1 46.6 49.7	MNR301** 67.4 63.8 52.7	CI603 60.4 57.1 58.5	PTR53 46.8 43.8 48.8	MNR215 26.5 24.6 28.5

Figure 4.2 The 3DDT calculated Power for Core 48A, 48A-MIX, and 48A-LEU

* LEU fuel assemblies in the mixed core.

** Old LEU fuel assemblies in core 48A and 48A-MIX.